Physical Properties of a New Type of Molten Electrolytes, $ZnCl_2$-$DMSO_2$

Min-Fong Shu, Hsin-Yi Hsu, and Chao-Chen Yang

Graduate School of Engineering Science & Technology (Doctoral Program), National Yunlin University of Science and Technology. 123, Sec. 3, University Road, Touliu, Yunlin, Taiwan, R. O. C.

Reprint requests to Min-Fong Shu; E-mail: g9010813@pine.yuntech.edu.tw

Z. Naturforsch. **58a,** 451 – 456 (2003); received May 12, 2003

In the present work some physical properties of binary zinc chloride-dimethylsulfone ($ZnCl_2$-$DMSO_2$) melts were investigated; the phase diagram was determined by Differential Scanning Calorimeter (DSC) and Thermogravimetric Analyzer (TGA) analyses; the electric conductivity was measured using a direct-current computerized method. The conductivities of the melts increased with increasing temperature and $DMSO_2$ content. There was a maximum of the conductivity at 40 mol% $ZnCl_2$; the conductivity was 0.00423 S/cm at 110 °C. The density of all the melts decreased with increasing temperature and $DMSO_2$ contents. The equivalent conductivities were given by $\Lambda = \kappa M_{\text{mix}}/\rho$, where M_{mix} is the mean equivalent weight. These equivalent conductivities were fitted by the Arrhenius equation, where the activation energies were 25.2, 34.6, 44.5, 53.7 kJ/mol for 40, 50, 60, 70 mol% $ZnCl_2$, respectively.

Key words: Direct-current Computerized Method; Archimedean Technique; Equivalent Conductivity; Activation Energy.

1. Introduction

Room temperature molten salts (RTMS) have drawn considerable attention [1, 2]. Best-known RTMS are melts containing $AlCl_3$. Hsu and Yang [3] have reported the conductivities of $AlCl_3$-BPC, $AlCl_3$-EMIC and $AlCl_3$-BTEAC, measured by a computerized direct current method. $AlCl_3$ is a strong Lewis acid so that melts containing $AlCl_3$ are easily affected by the environment. On the other hand, organic salt chlorides are good solvents of inorganic salts, but the preparation and conservation of organic salt chlorides is not so easy. Therefore more stable and convenient RTMS are wanted.

In the present study, zinc chloride-dimethylsufone ($ZnCl_2$- $DMSO_2$) was selected for investigation of its properties. Molten $CoCl_2$-$ZnCl_2$-BPC was used for the electrodeposition of amorphous Co/Zn alloy by Koura et al. [4]. In the literature, neither the conductivity nor the density of molten $ZnCl_2$-BPC is reported. Sun et al. [5] studied the electrodeposition of Zn, Co, Co/Zn and Cu/Zn alloys from the acidic $ZnCl_2$-EMIC melt. However, neither the conductivity nor the density of $ZnCl_2$-$DMSO_2$ melt is reported. $DMSO_2$ is a good solvent, stable at high temperature and able to dissolve numerous salts. A Raman study indicates that, when aluminum chloride is added to $DMSO_2$, peaks appear at 120, 179, and 347 cm^{-1}, which are assigned to $AlCl_4^-$ [6]. If a reaction occurs between $AlCl_3$ and $DMSO_2$, the coordination compound between Al^{3+} and $DMSO_2$ may be $[Al\text{-} (CH_3)_2SO_2]^{3+}$.

In the present work, the phase diagram of $ZnCl_2$-$DMSO_2$ melt is obtained by TGA and DSC analyses; the conductivities and densities of the melt are measured for the first time by a computerized method.

2. Experiment

2.1. Chemicals

$ZnCl_2$ (zinc chloride, Merck, anhydrous, 98%) and $DMSO_2$ (dimethylsulfone, Acros, 98%) were used in a dry glove box under a nitrogen atmosphere. The nitrogen had passed a drying column containing molecular sieves. The solutions were prepared in the dry glove box by mixing $DMSO_2$ with appropriate amounts of $ZnCl_2$ at 70 °C on a hot plate.

2.2. Phase Diagram

The phase diagram of the $ZnCl_2$- $DMSO_2$ melts was obtained by measuring the decomposition temperatures and the melting points. The thermal analyses were performed by TGA and DSC; the data of the

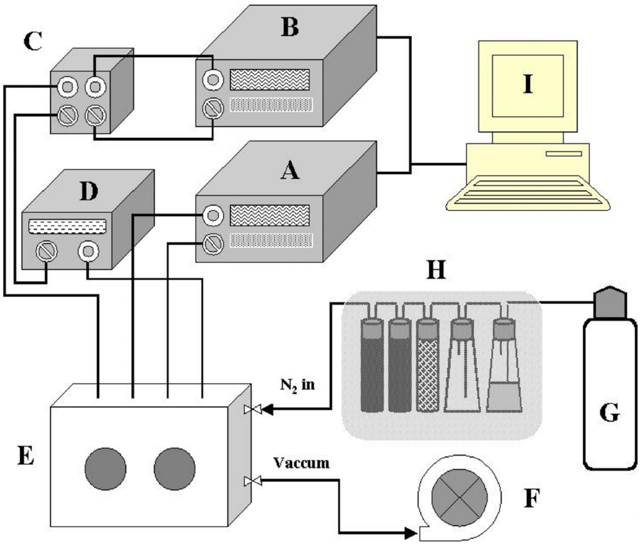

A. Multimeter 1
B. Multimeter 2
C. 10Ω standard resistor
D. DC Power supply
E. Glove box
F. Vacuum pump
G. N_2 gas
H. Gas purification
I. IBM-PC

Fig. 1. The apparatus for conductivity determination.

Table 1. Thermal analysis results of $ZnCl_2$-$DMSO_2$.

$ZnCl_2$/mol%	Melt point T_m/°C	Endothermic Enthalpy, ΔH/J g^{-1}	Decomposition temperature/°C
10	98.05	120.9	168.30
20	97.97	118.4	147.57
30	86.91	108.1	167.54
40	75.42	51.41	188.19
50	52.13	27.69	189.11
55	45.98	7.532	—
60	26.33	0.770	192.90
65	−39.15	2.445	—
70	−56.54	4.525	205.38
75	193.15	231.7	—
80	230.61	278.6	282.05

thermal analyses are shown in Table 1. The TGA analyses of the binary melts were carried out on a platinum tray which could be heated from 35 to 900 °C, with a heating rate of 20 K/min. A sealed aluminum disc was used for the DSC analysis, which was, at first, cooled to −60 °C by liquid nitrogen, and then the temperature was raised at a rate of 10 K/min.

2.3. Conductivity

The conductivity was determined by a computerized direct current method [3]. The computerized measurement system had a computer recording the data, as shown in Figure 1. The cell constant, evaluated with a 0.1 demal KCl solution at 25 °C was 286.82 cm^{-1}. The reference electrodes were an Ag-AgCl electrode and a platinum electrode. A direct current (Hewlett-Packard E3616A) of 2.5 A passed between the bipolar platinum electrodes. Two multimeters (Keithley, Model 2000) were employed for determining the potential drop at the two platinum electrodes, as shown in Figure 2. The electric conductivity of the $ZnCl_2$-$DMSO_2$ melt was measured as a function of temperature for four compositions.

2.4. Density

The density was measured based on the Archimedean principle [7–9], by determining the buoyancy of a platinum hammer immersed in the melt, which was suspended by a platinum wire (0.2 mmϕ) from one arm of a precise analytical balance (Mettler Toledo, AT261 Deltarange). The apparatus is schematically shown in Figure 3. The hammer volume of 2.4 cm^3 was measured in distilled water.

3. Results and Discussion

The phase diagram, determined by TGA and DSC analyses is shown in Figure 4. The decomposition temperatures (rhombuses) were measured by the TGA analysis, and the melting points (circles) by the DSC analysis. The range between the decomposition and melting points is thermally stable in the liquid state. The temperature range for measurement of the physical properties of 40, 50, 60, 70 mol% $ZnCl_2$ melts was chosen in the light of the phase diagram. The lowest

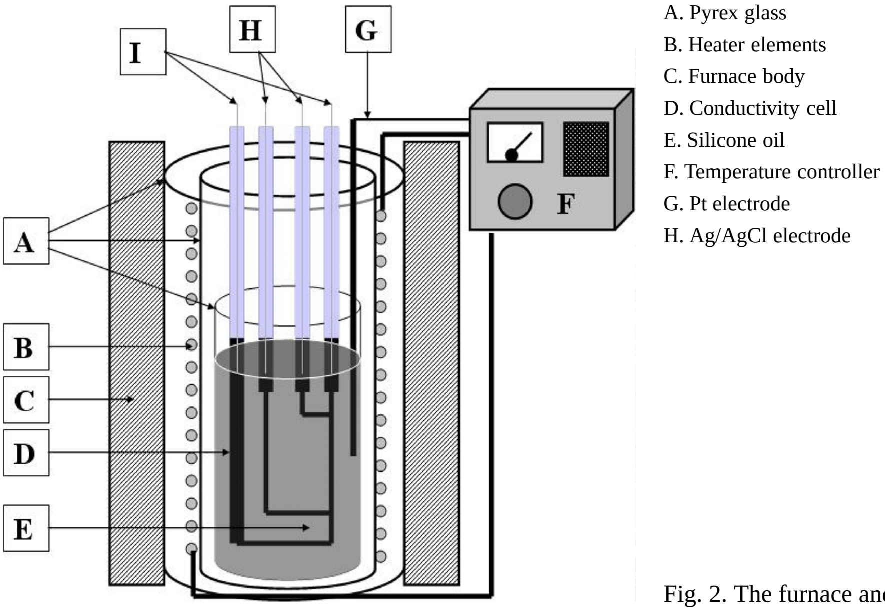

Fig. 2. The furnace and conductivity cell.

Table 2. Densities of molten $ZnCl_2$-$DMSO_2$.

$ZnCl_2$	$\rho = a' - b't$		R-squared	Temp. Range
per mol%	a'/g cm^{-3}	$b'/10^{-3}$ g cm^{-3}.$^{-1}$		in ℃
40	1.934	3.02	0.99890	90 – 110
50	2.191	4.50	0.99698	90 – 110
60	2.337	4.20	0.99570	90 – 110
70	2.526	4.77	0.99958	90 – 110

Table 3. Molar volumes of molten $ZnCl_2$-$DMSO_2$.

$ZnCl_2$	$V = a'' - b''t$		R-squared	Temp. Range
per mol%	a''/g cm^{3}mol^{-1}	$b''/10^{-2}$ cm^{3}mol^{-1}.$^{-1}$		in ℃
40	41.809	9.516	0.99853	90 – 110
50	34.570	12.032	0.99779	90 – 110
60	32.010	8.970	0.99668	90 – 110
70	28.429	8.619	0.99920	90 – 110

melting point of these compositions was −56.54 ℃ at 70 mol% $ZnCl_2$.

The densities of molten $ZnCl_2$-$DMSO_2$, shown in Fig. 5, follow the equation $\rho = \Sigma \rho_i x_i$, where x_i is the mole fraction of the species i. The temperature dependence of ρ at the four compositions is expressed by fitting an equation of the form $\rho = a' - b't$, where t is the temperature in ℃ and a' and b' are the parameters given in Table 2. The chart of the molar volume is shown in Fig. 6, and the forms $V = a'' + b''t$ obtained by fitting the equation are given in Table 3. The density could be influenced by complexing of the molecules or efficient packing of the ions [7]. An increase of the molar volume with increasing temperature was observed.

The relationship between the electric conductivity and the temperature at various compositions is shown in Figure 7. The experimental data were fitted to curves $\kappa = a + bt + ct^2$, where t is the temperature in ℃; the parameters a, b and c are given in Table 4. The slope of the conductivity decrease of 60 and 70 mol% $ZnCl_2$ melts between 60 and 85 ℃ is considerably smaller than that of 40 and 50 mol% $ZnCl_2$ melts. This is presumably because the $ZnCl_4{}^{2-}$ species increases with increasing amounts of $ZnCl_2$, which also causes an increase in the ionic interaction and the viscosities.

In the molten system $AlCl_3$-$DMSO_2$, the Raman spectra show that $AlCl_4^-$ is the main Al-containing species in the $DMSO_2$-based melts [10]. Assuming that a reaction occurs between $AlCl_3$ and $DMSO_2$, the following equilibrium is generally supposed:

$$AlCl_3 + n(CH_3)_2SO_2 = 3AlCl_4^- + Al[(CH_3)_2SO_2]_n^3 \tag{1}$$

The formation of $AlCl_4^-$ and $Al[(CH_3)_2SO_2]_n^{3+}$ ions is expected, where $AlCl_4^-$ is a stable compound of tetrahedral coordination. However, if a reaction similar to (1) occurs, some of the zinc will be present as a complex cation [6]. Further, the Raman spectra of the molten systems $ZnCl_2$-MCl (M=Li, K) show that the coordination complexes of $ZnCl^+$, $ZnCl_3^-$ (planar or pyramidal), $ZnCl_4^{2-}$ (tetrahedral), and $ZnCl_6^{4-}$ (octahedral) are present [11]. In the case of $ZnCl_2$-$DMSO_2$,

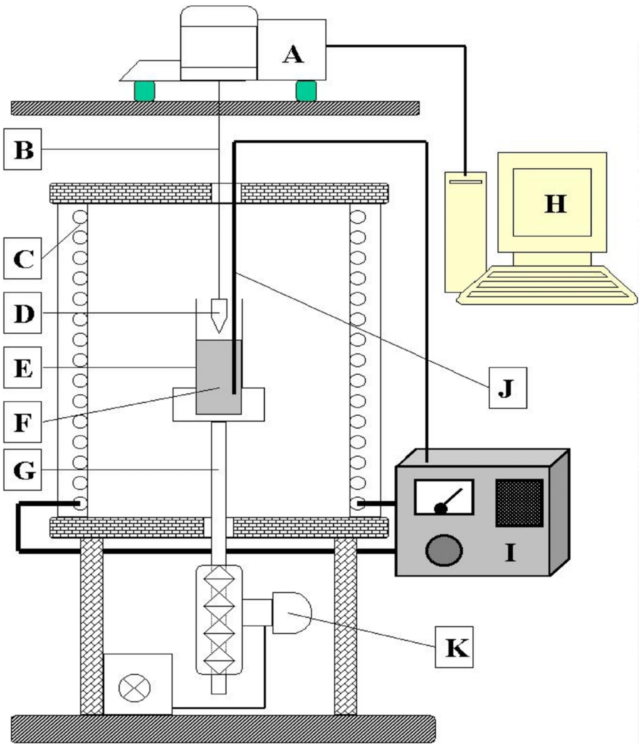

A. Analytical balance
B. Pt suspension wire
C. Ni-Cr Pyrex tube furnace
D. Platinum hammer
E. Platinum cell
F. Molten salts
G. Cell supporter
H. Personal computer
I. Temperature controller
J. Thermocouple
K. Auto.movable stand

Fig. 3. Apparatus for measurement of the molten salts density.

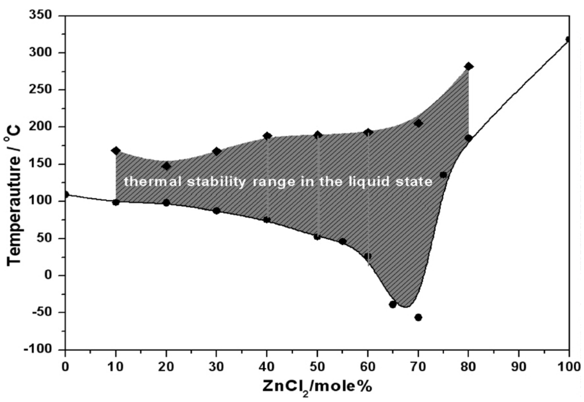

Fig. 4. Phase diagram of $ZnCL_2$-$DMSO_2$.

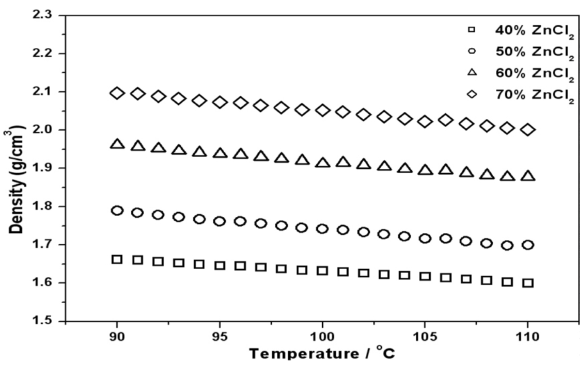

Fig. 5. Density of $ZnCL_2$-$DMSO_2$ melts at four compositions as functions of the temperature.

the ionic reaction between $ZnCl_2$ and $DMSO_2$ may be similar to that in the $AlCl_3$-$DMSO_2$ system:

$$2ZnCl_2 + n(CH_3)_2SO_2 = ZnCl_4^{2-} + Zn[(CH_3)_2SO_2]_n^{2+} \tag{2}$$

What kinds of Zn-containing species exist must depend on complex formation of higher coordination numbers. Non-complexing ionic species must be dominating in transport properties, such as the ionic conductivity. It is also suggested that the information obtained from the spectra and the viscosity reflects the ionic structure of the liquid. The movement of ions increases with temperature, and the highest conductivity is given at 40 mol% $ZnCl_2$ among compositions investigated, as shown in Figure 7. This demonstrates that the increase of $DMSO_2$ will increase not only the molar volume but also the ionic mobility.

Table 4. Electric Conductivities of molten $ZnCl_2$-$DMSO_2$.

$ZnCl_2$ per mol%	$a/10^{-4}\,\mathrm{S\,cm^{-}1}$	$b/10^{-5}\,\mathrm{S\,cm^{-1}.^{-1}}$	$c/10^{-7}\,\mathrm{S\,cm^{-1}.^{-2}}$	R-squared	Temp. Range in °C
	$\kappa = a + bt + ct^2$				
40	−6.905	1.414	2.773	0.99996	60 – 110
50	0.811	−2.492	5.563	0.99994	60 – 110
60	23.20	−8.923	9.180	0.99988	60 – 110
70	40.70	−13.027	11.053	0.99975	60 – 110

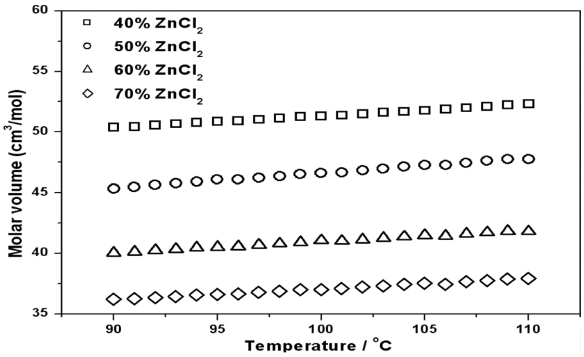

Fig. 6. Molar volume of $ZnCL_2$-$DMSO_2$ melts at four compositions as functions of the temperature.

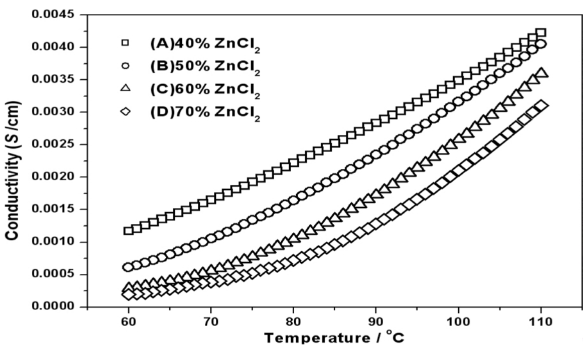

Fig. 7. Electric conductivity of $ZnCL_2$-$DMSO_2$ melts at four compositions as functions of the temperature.

These equivalent conductivities can be fitted by Arrhenius-type equations,

$$\kappa = \kappa_0 \exp(-E_\kappa/RT) \text{ and } \Lambda = \Lambda_0 \exp(-E_\Lambda/RT);$$

plots of the data for the $ZnCl_2$-$DMSO_2$ melts are shown in Figure 8. The parameters of the activation energies for the isotherms of the equivalent conductivity and the electric conductivity are given in Table 5. Generally, the salt with a low lattice energy tends to show a high ionic migration, because the low dissociation energy increases the number of free ions [3]. Thus, the 40 mol% $ZnCl_2$ melt has the lowest equivalent conductivity and electric conductivity activation energies among the various compositions. Both activation energies are closely linked and E_κ is always greater than E_Λ in the $ZnCl_2$-$DMSO_2$ system. The similarity between E_κ and E_Λ is indicative for ionic packing or complex formation in the melt. In the case of $ZnCl_2$-$DMSO_2$, the ratio of E_κ/E_Λ is 1 – 1.3 at 90 – 110 °C.

Table 5. Activation enrgies from Arrhenius fits of the conductivity and equivalent conductivity of the $ZnCl_2$-$DMSO_2$ melt.

$ZnCl_2$/mol%	$\kappa = k_0 \exp(-E_\kappa/RT)$ $E_\kappa/\mathrm{kJ\,mol^{-}1}$	$\Lambda = \Lambda_0 \exp(-E_\Lambda/RT)$ $E_\Lambda/\mathrm{kJ\,mol^{-}1}$
40	26.948	25.230
50	39.667	34.588
60	54.082	44.473
70	59.934	53.749

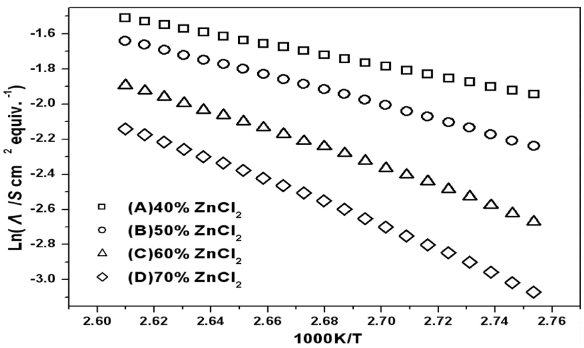

Fig. 8. Arrhenius plots of the equivalent conductivity of $ZnCL_2$-$DMSO_2$ melts at four compositions.

4. Conclusion

The phase diagram, electric conductivity and density of $ZnCl_2$-$DMSO_2$ melts have been measured at 40, 50, 60 and 70 mol% $ZnCl_2$.

(1) The electric conductivities have a maximum at 40 mol% $ZnCl_2$ at 60 – 110 °C.

(2) The activation energies (E_κ and E_Λ) have the lowest values at 40 mol% $ZnCl_2$ at 90 – 110 °C.

(3) The highest molar volume and the lowest density are observed for 40 mol% $ZnCl_2$ at 90 – 110 °C. The density and molar volume could be influenced by the complex formation of the molecules or efficient packing of the ions.

(4) The ionic migration of the four compositions is in the order: 40, 50, 60, 70 mol% $ZnCl_2$.

Acknowledgements

This work was financially supported by the Nation Science Council, the Republic of China, under contract No. NSC 90-2214-E-224-008.

[1] S. Takahashi, N. Koura, S. Kohara, M. L. Saboungi, and L. A. Curtiss, Plasmas and Ions, **2**, 91 (1999).
[2] Y. Zhao and T. J. VanderNoot, Electrochim. Acta, **42**, 3 (1997).
[3] H. Y. Hsu and C. C. Yang, Z. Narturforsch. **56a**, 670 (2001).
[4] N. Koura, T. Endo, and Y. Idemoto, J. Non-Cryst. Sol. **205 – 207**, 650 (1996).
[5] P. Y. Chen, M. C. Lin, and I. W. Sun, J. Electrochem. Soc. **147**, 3350 (2000).
[6] T. Hitato, J. Fransaer, and J. P. Celis, J. Electrochem. Soc. **148**, C280 (2001).
[7] D. L. Thomas, J. Y. Cherng, and D. N. Bennion, J. Electrochem. Soc. **135**, 2674 (1988).
[8] G. Pedro Smith and Guy F. Petersen, J. Chem. Eng. Data, **6**, 493 (1961).
[9] J. Ye and Y. Sahai, Mat. Trans. JIM, **37**, 170(1996).
[10] L. Legrand, A. Tranchant, and R. Messina, Inorg. Chem. **35**, 1310 (1996).
[11] R. B. Ellis, J. Electrochem. Soc. **113**, 485 (1966).